Journal of the Korean Physical Society, Vol. 59, No. 4, October 2011, pp. 2792∼2796

Anomalous Weak Ferromagnetism in Electron-doped $Nd_{1-x}Sr_xMnO_3$ ($0.50 \leq x \leq 0.62$) Thin Films

Pawan Kumar*
National Physical Laboratory (CSIR), Dr. K. S. Krishnan Marg, New Delhi-110012, India and
Department of Physics and Materials Science & Engineering,
Jaypee Institute of Information Technology (Deemed University), Noida-201307, Uttar Pradesh, India

Ravikant Prasad, Avanish Kumar Srivastava and Hari Krishna Singh
National Physical Laboratory (CSIR), Dr. K. S. Krishnan Marg, New Delhi-110012, India

Rakesh Kumar Dwivedi
Department of Physics and Materials Science & Engineering,
Jaypee Institute of Information Technology (Deemed University), Noida-201307, Uttar Pradesh, India

Mangala Prasad Singh
Department of Physics, Brock University, 500 Glenridge Ave., St. Catharines L2S3A1, Canada

(Received 13 May 2011, in final form 29 August 2011)

In the present work, we demonstrate that an anomalous weak ferromagnetism occurs in the composition range $0.50 \leq x \leq 0.62$ in nanostructured thin films of $Nd_{1-x}Sr_xMnO_3$ (NSMO). Nanocrystalline thin films of overdoped manganite $Nd_{1-x}Sr_xMnO_3$ ($x \sim 0.50$, 0.55, 0.60, and 0.62) are grown on single-crystal $LaAlO_3$ (001) substrates by using a nebulized chemical spray pyrolysis technique. These single phase films possess an average crystallite size ∼15 nm, and the width of the grain boundaries is ∼1 – 2 nm. In the composition range $0.50 \leq x \leq 0.62$, the ground state of NSMO is an A-type antiferromagnetic (AFM) metallic state. However, in the present films, a broad paramagnetic (PM)-to-ferromagnetic (FM) transition is observed in all the compositions, at $T_C \sim 226$ K for $x = 0.50$ and at 235 K for rest of the samples. All the films show a well-defined M-H hysteresis loop at 5 K. The coercivity (H_C) of these films is much larger than those having compositions in the range $0.35 < x < 0.45$. For $x = 0.50$ (0.62), the films H_C = –1210 (–1484) Oe and +1162 (+1476) Oe. The asymmetry in the coercivity suggests the presence of a weak exchange bias effect in these films. The FM ground state in these films is observed to have a smaller magnetic moment per Mn atom than the expected full moment from the rigid model; we term this as a weak ferromagnetic (WFM) state arising due to the destabilization of the AFM ordering. We propose a possible scenario based on the combined effect of spin reorganization and enhanced orbital disordering in nanosized manganites to explain the observed anomalous weak ferromagnetism in the A-type AFM spin ordered region.

PACS numbers: 75.75.+a
Keywords: Manganite, Thin films, Anomalous weak ferromagnetism, Microstructure
DOI: 10.3938/jkps.59.2792

I. INTRODUCTION

Recently, several experimental and theoretical studies have been focused on the exploration of the grain size effect on the functional properties of doped perovskite manganites [1–10]. These studies clearly highlight the significance of broken exchange bonds between the surface Mn cations and their likely impact on the magnetic properties. In nano-manganites, when the size is reduced below 100 nm, the charge and the orbitally ordered (CO-OO) ground state with antiferromagnetic (AFM) spin order have been shown to become unstable, and this gives rise to a ferromagnetic (FM) ground state [3,11]. Size-induced transition from the AFM/CO state to the weak ferromagnetic (WFM) state was observed in both nanowires [3] and nanoparticles [4]. Lu *et al.* [11] showed that destabilization of the AFM-CO state and the formation of a FM order could result in an enhancement

*E-mail: pawangk@yahoo.co.in; Fax: +91-120-2400986

of the magnetization by two orders of magnitude. The WFM ground state resulting in nanomanganites from the destabilization the AFM ground state has been regarded to be direct consequence of size reduction because when the size is small enough (*e.g.*, 20 nm), the effect of surface spin disordering becomes more evident. However, a WFM induced by the destabilization of the AFM order has also been reported in single crystals [12,13], as well as epitaxial thin films [14]. This suggests that the evolution of the WFM state out of the AFM-CO state cannot be attributed to downsizing to nanometric scale alone and that some additional effects, such as orbital disordering, may also be equally important [13–17].

Material downsizing can have a more dramatic effect in the vicinity of bicritical regions in manganites. Among the manganites, $Nd_{1-x}Sr_xMnO_3$ (NSMO) possesses several bicritical regions [13]. In the case of NSMO, the AFM phase spans the whole overdoped region ($0.50 \leq x \leq 1$) wherein the A-type AFM (antiferromagnetically coupled two- dimensional ferromagnetic order) occurs up to $x \sim 0.63$. Above that, C-type AFM (antiferromagnetically coupled one-dimensional ferromagnetic order) takes over. The phase boundary at $x \sim 0.63$ that separates the A- and the C-type AFM phases has been shown to possess a fairly large FM contribution [12–14]. In single crystals and epitaxial thin films [12–14], this FM and the associated transition has been attributed to the strong orbital fluctuation/disorder in the proximity of the A-C phase boundary. Nanocrystalline thin films, by virtue of their large surface-to-volume ratios and local epitaxy, can provide an additional degree of freedom to tune and to complement the WFM at the A-C AFM phase boundary in NSMO. However, nanocrystalline thin films of this material have not been investigated so far.

In the present work, we show that the A-AFM phase in nanocrystalline thin films (having crystallite size <20 nm) of overdoped NSMO ($x \sim 0.60$ – 0.62) can be destabilized, resulting in the occurrence of a FM phase. In addition to the small magnetic moment, the remanence, the large coercivity, the exchange bias (EB) effect suggests the presence of a FM phase.

II. EXPERIMENTS

The nanocrystalline thin films (∼300nm thickness) have been prepared on single- crystal $LaAlO_3$ (100) substrates by using the well known nebulized chemical spray pyrolysis technique [18]. Films were deposited at 300 °C by spraying a homogeneous 0.2molar aqueous solution of Nd, Sr and Mn nitrates. The cationic ratio was *Nd/Sr/Mn = 1-x/x/1* (x = 0.50, 0.55, 0.60, and 0.62). All films were annealed in air at 920 °C for two hours. The structural and the microstructural characterizations were done by using powder X-ray diffraction (XRD, X'Pert PRO PANalytical, CuK_α radiation), scanning electron microscopy (SEM) and high resolution transmission electron microscopy (HRTEM, FEI Tecnai G^2 F30 STWIN, 300 kV FEG) with energy dispersive X-ray spectroscopy (EDS). We measured the DC magnetization in the temperature range 4 – 300 K by using a superconducting quantum interference device (SQUID) magnetometer (MPMS-XL/quantum design).

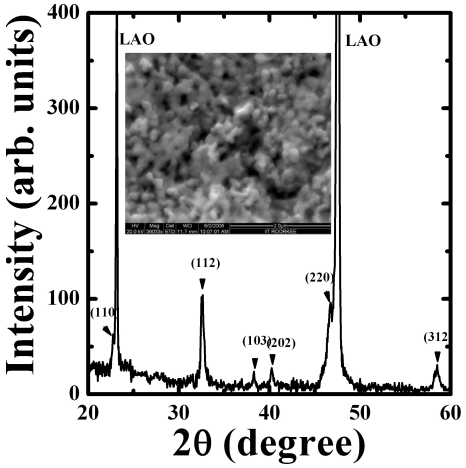

Fig. 1. Representative XRD pattern of a NSMO film (x ∼ 0.62). The SEM picture in the inset shows the surface morphology of this film.

III. RESULTS AND DISCUSSION

A typical θ-2θ XRD pattern for the $x = 0.62$ film is shown in Fig. 1. The XRD pattern is characterized by well-sharp reflections dominantly along ($hk0$) and ($hk2$). It clearly shows that the films are textured and polycrystalline in nature. Irrespective of the compositions, our detailed studies revealed that the films were polycrystalline and possessed the orthorhombic symmetry (space group/Ibmm). The crystal structure of the films was found to be orthorhombic. The unit cell lattice parameters were a = 5.492 Å, b = 5.473 Å, and c = 7.764 Å. No impurities and secondary phases were observable in the XRD data. The cationic composition, investigated by EDS carried out at several places on the films ($x \sim 0.62$), revealed that Nd/Sr/Mn ≈ 0.38/0.62/0.95. A small variation of the compositions in the range $x \sim 0.50$ – 0.62 had no observable effect on the structure of these films.

The surface microstructure of the films, as revealed by SEM, was found to consist of nanometric grains. A representative micrograph showing the surface morphology of the $x \sim 0.62$ film is inserted in the inset of Fig. 1. A detailed HRTEM experiment was conducted to explore the nano- and sub-nano-scale microstructures of the $x \sim$ 0.62 thin films. In general, nanocrystallites of about 10 to 20 nm in size were randomly distributed throughout the film's microstructure (Fig. 2(a)). These nanocrystallites were mostly surrounded by grain boundaries of relatively thin size, *viz.* 1 to 2 nm in thickness. These films

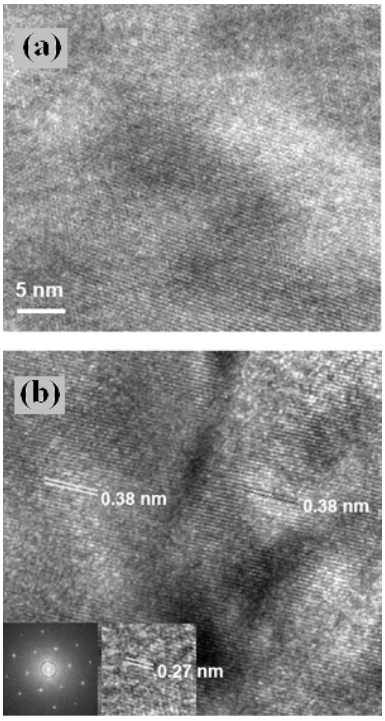

Fig. 2. HRTEM micrograph showing a typical microstructure of a NSMO film ($x \sim 0.62$). Disordered regions sandwiched between the crystalline ones can be easily discerned in both the micrographs (a) and (b). The major lattice spacing (d = 0.386 nm) has been marked in (b). The less frequently observed interplaner separation has been inserted as an inset in (b). The SAED pattern corresponding to the microstructure (b) is shown in the inset.

were also composed of amorphous regions in which the nanocrystallites were embedded. The amorphous regions and the grain boundaries (again amorphous) normally coexisted. The amorphous regions can be regarded as highly disordered regions of the grain boundary in these nanocrystalline films. Lattice imaging of these nanocrystallites revealed that most of these crystals were composed of (110) planes of an orthorhombic structure. The interplanar separation between two planes was d_{110} = 0.38 nm. A corresponding selected area electron diffraction pattern is displayed as an inset in Fig. 2(b). Normally, we do not observe the growth of any other set of planes in these nanocrystallites, confirming the preferred growth. However, in a few regions, the nanocrystallites grown in other directions were also revealed as illustrative examples, the lattice planes (*hkl*: 112) are marked in the microstructure (see the inset in Fig. 2(b)). The lattice spacing was found to be d_{112} = 0.27 nm. These observations are clear evidences that the whole film is composed of a quantum-well-type structure, where the low-energy nanocrystallites are surrounded by high energy grain boundaries (disordered structure).

The temperature dependence of the remanent magnetization of all the films shows a broad FM transition

Table 1. Values of T_C, M_r, M_S, and H_C for $Nd_{1-x}Sr_x MnO_3$ ($0.50 \leq x \leq 0.62$) thin films on LAO (001) single-crystal substrates.

x	T_C (K)	M_r (μ_B/Mn)	M_s (μ_B/Mn)	(−)H_C (Oe)	(+)H_C (Oe)
0.50	226	3.55	5.23	1210	1162
0.55	235	2.64	4.74	1097	1067
0.60	235	0.81	1.53	1359	1326
0.62	235	0.63	1.17	1484	1476

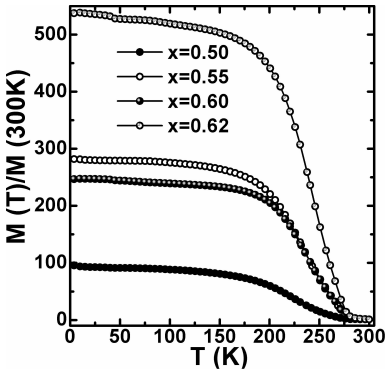

Fig. 3. Temperature dependence of the remanence (measured at H = 500 Oe) of $Nd_{1-x}Sr_xMnO_3$ thin films. For comparison the magnetization data have been normalized to the room-temperature value.

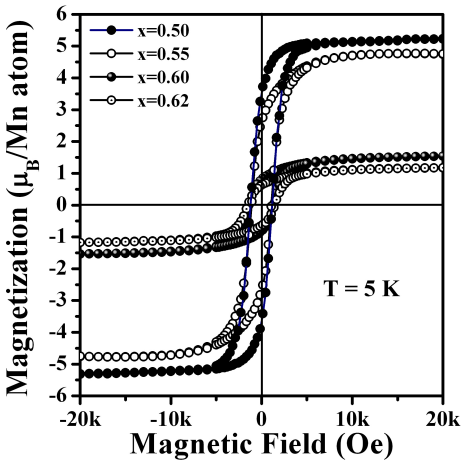

Fig. 4. (Color online) Variation of the magnetic field with magnetic field (measured at T = 5 K) of $Nd_{1-x}Sr_xMnO_3$ thin films.

(Fig. 3); for comparison, the magnetization data have been normalized to the room temperature value. In the present films, the remanence (M_r) is much larger than the values reported for single crystals and epitaxial thin films of similar compositions [13,14]. The M-H loop for all the films recorded at T = 5 K is shown in Fig. 4. Although the film shows a well-developed M-H loop, the FM ground state appears to be different in many re-

spects from that of the optimally-doped NSMO ($x \sim 0.30 - 0.45$) [15]. Further, the irreversibility of the M-H loop in these films vanishes at a much higher field $H_S \sim 18$ kOe. The observed saturated magnetization (M_S) in the present case is much lower, and the saturation field is significantly larger than that observed in optimally-hole-doped conventional manganites [15]. One possible reason for the large coercive applied magnetic field (H_C) and saturated applied magnetic field (H_S) in the present case could be the pinning of magnetic domains by the grain boundaries/amorphous regions. In the present overdoped NSMO ($x \sim 0.62$) films, the coercivity $H_C \sim$ –1484 and +1476 Oe. This is nearly an order of magnitude higher than that of the manganites ($H_C \sim 100 - 200$ Oe) in conventional hole-doped manganites having optimum hole doping (20 – 40%) [15]. The asymmetry in the H_C values, although small, suggests the presence of a weak exchange bias (EB) effect with a small EB field $H_{EB} \sim 50$ Oe. Since the EB is caused by the formation of FM-AFM interfaces, this also confirms the presence of both FM and AFM phases. The magnetic moment is found to be very sensitive to the doping (x). When the x (Sr content) is reduced slightly from $x \sim 0.62 - 0.60$, the M drops to about half the value at $x \sim 0.62$, but the PM-FM transition remains nearly the same [Fig. 3]. The values of T_c, M_r, M_s, and H_c for all the films are given in Table 1. This observation is in agreement with the magnetization data for single crystals of similar compositions reported by Akahoshi *et al.* [13] . Interestingly, the exchange bias effect observed at $x \sim 0.62$ gets diluted when the Sr content is reduced to $x \sim 0.60$, suggesting a reduced FM phase fraction. In these films, the coercivity is found to be $H_C \sim$ –1359 and +1326 Oe, giving a negligible $H_{EB} \sim 10$ Oe.

In manganites, the appearance of FM behavior in AFM region is not surprising. In nano-manganites with an AFM ground state (such as the present nanocrystalline thin films), the superexchange interaction that drives AFM is diluted by the surface disorder [6,16,17,19,20]. This induces a reorganization of the disordered surface spins and has recently been explained in terms of the core-shell model [19,20]. In the core-shell model, the magnetization has been expressed as,

$$M = \alpha M_{shell} \sum_{ij} \cos\theta_{ij} + (1-\alpha) M_{core} \qquad (1)$$

the shell thickness 'α', which can be regarded as a measure of the surface disorder, increases with decreasing crystallite size. The angle between two spins i and j (θ_{ij}) is 180° for the cores, but for the shells, it can attain any value $\theta_{ij} < 180°$. Further, we suggest that as the boundary between the core and the shell may not be sharp, θ_{ij} will show a negative gradient away from the inner part of the shells (that is, θ_{ij} will be closer to 180° on the inner part of the shells, but on the outer part, it will have the lowest value). Since in the present study, the average crystallite size is about 15 nm, the shell contribution is expected to be significant. In other words, as the grain size scales down, the effective FM and AFM exchange interactions J_{FM} and J_{AFM} are expected to be renormalized. Within the core, the J_{AFM} prevails, and the spin ordering is AFM. The outer shell should, strictly speaking, be spin disordered and less stable than both AFM and FM. One natural way, to minimize or reduce the energy to achieve a stable configuration for this spin disordered shell around the AFM core would be through reorganization of the spin order. The emergent spin order is in the form of a FM shell around the AFM core. However, the spins on the outermost regions are expected to be more parallel than those located on the inner part of the shell. The occurrence of the FM shell results in the formation of natural AFM/FM interfaces that also causes the EB effect. In nanosized samples, coexistence of three magnetic components, *viz.*, AFM component cores of nanoparticles, a weak FM component due to reorganized surface magnetism, and a magnetic-field-induced weak FM component of the cores, is possible. Thus, in one possible scenario, this is phase separation on a nanoscale, where the weak FM component can be regarded as a nanoscale inhomogeneity present in an AFM matrix comprised of grain cores. However, as seen in the M-T and the M-H results, the relatively large magnetic moment and the reasonably well-developed FM transition are different from the WFM observed in other overdoped/electron-doped manganites [11,13,14,20].

At this point, we would like to emphasize that the orbital order (OO) [16,17], which is also affected by the reduced crystallite size, may play a very important role in the stabilization of the FM component. In manganites, it is generally accepted that orbital disordering, *i.e.*, the mixed state of $3d(z^2 - r^2)$ and $3d(x^2 - y^2)$ orbitals, stabilizes FM phases [14–17]. At the A- to C-AFM phase boundary at $x \sim 0.62 - 0.63$, the presence of competing $3d(x^2 - y^2)$ and $3d(z^2 - r^2)$ orbital orders should cause strong orbital fluctuations that may be controlled by crystallite size effects and the degree of polycrystalline disorder. The important role of orbital fluctuations is also indicated by the sharp decrease in the value of the magnetic moment when the Sr concentration is lowered from the value corresponding to the A-C AFM phase boundary ($x \sim 0.62 - 0.63$). Hence, in nanosized overdoped NSMO, the FM phase may be due to the combined effect of reduced crystallite size and orbital disordering/fluctuations on the spin reorganization at the crystallite shells.

IV. CONCLUSION

In conclusion, overdoped $Nd_{1-x}Sr_xMnO_3$ ($x \sim 0.50 - 0.62$) polycrystalline thin films having an average crystallite size of ∼15 nm have been studied in relation to their magnetic properties. These films exhibit anomalous ferromagnetism that is very sensitive to even small variations in the x-value. In addition to the significant

magnetic moment, the remanence and the large coercivity, the exchange bias (EB) effect suggests the presence of a FM phase. The occurrence of this FM phase has been qualitatively explained in terms of spin reorganization due to reduced crystallite size and enhanced orbital disordering.

ACKNOWLEDGMENTS

The authors are grateful to the Director, NPL, for encouragement and support. Pawan Kumar thanks CSIR for the senior research fellowship. The authors are also grateful to Dr. G. D. Varma (IIT-R) for some measurements and discussion.

REFERENCES

[1] Y. Tokura and Y. Tomioka, J. Magn. Magn. Mater. **200**, 1 (1999).
[2] F. Chen, H. W. Liu, K. F. Wang, H. Yu, S. Dong, X. Y. Chen, X. P. Jiang, Z. F. Ren and J-M. Liu, J. Phys. Condens. Matter **17**, L467 (2005).
[3] S. S. Rao, K. N. Anuradha, S. Sarangi and S. V. Bhat, Appl. Phys. Lett. **87**, 182503 (2005).
[4] S. S. Rao, S. Tripathi, D. Pandey and S. V. Bhat, Phys. Rev. B **74**, 144416 (2006).
[5] Z. Q. Wang, F. Gao, K. F. Wang, H. Yu, Z. F. Rena and J-M. Liu, Mater. Sci. Eng., B **136**, 96 (2007).
[6] A. Biswas and I. Das, Phys. Rev. B **74**, 172405 (2006).
[7] A. Biswas, I. Das and C. Majumdar, J. Appl. Phys. **98**, 124310 (2005).
[8] K. S. Shankar, S. Kar, G. N. Subbanna and A. K. Raychaudhuri, Solid State Commun. **129**, 479 (2004).
[9] T. Zhang, C. G. Jin, T. Qian, X. L. Lu, J. M. Bai and X. G. Li, J. Mater. Chem. **14**, 2787 (2004).
[10] S. Dong, F. Gao, Z. Q. Wang, J-M. Liu and Z. F. Ren, Appl. Phys. Lett. **90**, 082508 (2007).
[11] C. L. Lu, S. Dong, K. F. Wang, F. Gao, P. L. Li, L. Y. Lv and J-M. Liu, Appl. Phys. Lett. **91**, 032502 (2007).
[12] M. Nagao *et al.*, J. Phys. Condens. Matter **19**, 492201 (2007).
[13] D. Akahoshi, R. Hatakeyama, M. Nagao, T. Asaka, Y. Matsui and H. Kuwahara, Phys. Rev. B **77**, 054404 (2008).
[14] R. Prasad, M. M. Singh, P. K. Siwach, P. Fournier and H. K. Singh, Europhys. Lett. **84**, 27003 (2008).
[15] Y. Tokura, Rep. Prog. Phys. **69**, 797 (2006).
[16] G. V. Pai, Phys. Rev. B **63**, 064431 (2001).
[17] A. Taraphder, J. Phys. Condens. Matter **19**, 125218 (2007).
[18] H. K. Singh, P. K. Siwach, N. Khare and O. N. Srivastava, J. Phys. D: Appl. Phys. **33**, 921 (2000).
[19] R. N. Bhowmik, R. Nagarajan and R. Ranganathan, Phys. Rev. B **69**, 054430 (2004).
[20] T. Zhang, T. F. Zhou, T. Qian and X. G. Li, Phys. Rev. B **76**, 174415 (2007).